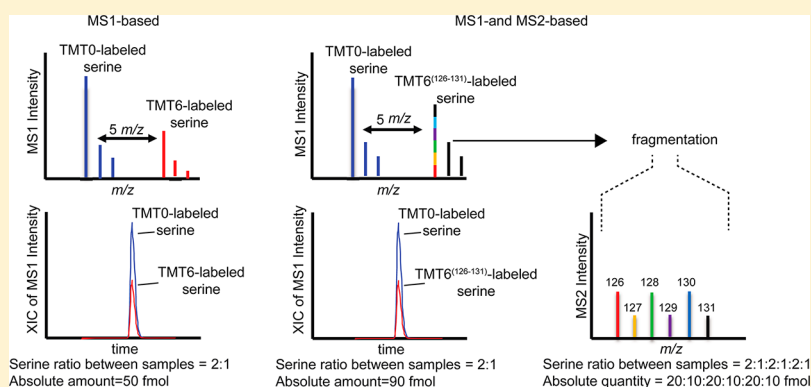


# Combining Amine Metabolomics and Quantitative Proteomics of Cancer Cells Using Derivatization with Isobaric Tags

J. Patrick Murphy,\* Robert A. Everley, Jonathan L. Coloff, and Steven P. Gygi\*

Department of Cell Biology, Harvard Medical School, Boston, Massachusetts 02115, United States

## S Supporting Information



**ABSTRACT:** Quantitative metabolomics and proteomics technologies are powerful approaches to explore cellular metabolic regulation. Unfortunately, combining the two technologies typically requires different LC-MS setups for sensitive measurement of metabolites and peptides. One approach to enhance the analysis of certain classes of metabolites is by derivatization with various types of tags to increase ionization and chromatographic efficiency. We demonstrate here that derivatization of amine metabolites with tandem mass tags (TMT), typically used in multiplexed peptide quantitation, facilitates amino acid analysis by standard nanoflow reversed-phase LC-MS setups used for proteomics. We demonstrate that this approach offers the potential to perform experiments at the MS1-level using duplex tags or at the MS2-level using novel 10-plex reporter ion-containing isobaric tags for multiplexed amine metabolite analysis. We also demonstrate absolute quantitative measurements of amino acids conducted in parallel with multiplexed quantitative proteomics, using similar LC-MS setups to explore cellular amino acid regulation. We further show that the approach can also be used to determine intracellular metabolic labeling of amino acids from glucose carbons.

Cellular metabolic regulation is a key aspect in the biology of cancer, diabetes, and many other diseases. As a result of the high complexity of cell metabolism, systems-level analyses are crucial in understanding its regulation, involving both quantitative proteomic and metabolic measurements.<sup>1</sup> Amino acids are a particularly important class of metabolites since they are key intermediates between carbon and nitrogen metabolism supporting protein synthesis and many other anabolic processes in cells. Dysregulated amino acid metabolism is associated with a number of infantile genetic diseases such as phenylketonuria<sup>2</sup> and maple syrup urine disease<sup>3</sup> and has recently been shown to be involved in certain cancers.<sup>4</sup> Unfortunately, mass spectrometry analysis of amino acids is not directly amenable to the reversed-phase LC-MS setups commonly used for proteomics,<sup>5</sup> making parallel proteomic and metabolomic measurements difficult. Even with many other types of LC-MS analyses, such as with hydrophilic interaction chromatography (HILIC) and ion-pairing reversed-phase chromatography, amino acids remain difficult to analyze because of their high polarity, poor ionization efficiency, and high structural similarity.<sup>5</sup>

Chemical derivatization is a powerful approach to analyze classes of molecules by mass spectrometry providing increased sensitivity and chromatographic separation during LC-MS.<sup>5</sup> Although derivatization approaches are limited to metabolites carrying specific functional groups, isotope enrichment of the chemical tag can be used to derivatize standards, eliminating the need for an isotopically enriched standard for each compound. Chemical labeling also typically increases the ionization efficiency and chromatographic resolution of the compound and increases the mass to a higher, cleaner  $m/z$  range.

A common derivatization strategy for amine metabolites, including amino acids is the use of NHS ester-based reaction chemistry followed by LC-MS analysis. This strategy has previously been employed to measure amine metabolites using tags designed for peptide quantification; iTRAQ,<sup>6</sup> AcQ,<sup>7</sup> and DiART.<sup>8,9</sup> The NHS ester-based, amine-derivatizing, tandem mass tag (TMT) reagents are also available for peptide analysis

Received: January 13, 2014

Accepted: March 10, 2014

Published: March 10, 2014

for multiplexed quantitative proteomics, whereby their addition to a peptide maintains a nominal mass for tagged peptides from multiple samples but fragmentation produces unique isotopic reporter ions for multiplexed sample quantitation.<sup>10</sup> These reagents are set apart from previous isobaric tags by recent improvements allowing up to 10 unique reporter ions distinguishable by high-resolution mass spectrometry.<sup>15</sup> Here, we have employed TMT reagents to facilitate reversed-phase LC-MS analysis of amino acids. We demonstrate the utility of the approach for MS1- and MS2-based quantitation, whereby MS2-based quantitation facilitates multiplexed analysis such that amino acids can be measured in parallel with novel 10-plex TMT-based quantitative proteomics. We further demonstrate a combination of metabolic and TMT labeling to measure glucose flux to amino acids in breast cancer cells with amplified serine biosynthesis.

## ■ EXPERIMENTAL SECTION

**Cell Culture.** MCF-7, MDA-MB-468, MDA-MB-231, and SKBR3 cells were maintained in DMEM (Invitrogen, Carlsbad, CA) containing 10% FBS (Invitrogen, Carlsbad, CA). MCF10A cells were maintained in DMEM/F12 containing 5% horse serum, 2 ng/mL epithelial growth factor (R&D Systems, Minneapolis, MN), 500 ng/mL hydrocortisone (Sigma, St. Louis, MO), 100 ng/mL cholera toxin (Sigma, St. Louis, MO), and 10  $\mu$ g/mL insulin (Sigma, St. Louis, MO). Cells were subcultured by rinsing with PBS and detaching with 0.5% trypsin-EDTA (Invitrogen, Carlsbad, CA). For experiments measuring amino acids during glucose withdrawal or cell line comparison experiments, cells were plated in 6-well plates at a density of  $2 \times 10^5$  cells per well. For glucose withdrawal experiments, cells were plated in high-glucose (25 mM) DMEM, allowed to adhere overnight, and then switched to media containing either 10 or 1 mM glucose for 24 h. For multiplexed proteomics comparison of 5 cancer cell lines, all cell lines were plated in 15 cm plates at  $5 \times 10^6$  cells per plate and grown to 80% confluency. For <sup>13</sup>C-glucose labeling experiments, cells were plated in high glucose DMEM overnight and then switched to fully labeled <sup>13</sup>C-glucose (Cambridge Isotope Laboratories, Tewksbury, MA) for 48 h.

**Metabolite Extraction, Labeling, and Glucose/Lactate Analysis.** For media analysis, media was removed from cells, diluted 4 $\times$  with cold methanol, and centrifuged at 13 000g for 5 min, and the supernatant extract was used for labeling. For intracellular analysis, cells were rinsed with PBS and extracted by scraping in 300  $\mu$ L of cold ( $-80^\circ\text{C}$ ) 80% methanol and then centrifuged at 13 000g for 5 min. All TMT labeling (standards, media extract, or intracellular extract) was achieved by mixing 30  $\mu$ L of standard or extract with 70  $\mu$ L of 50 mM TEAB and 10  $\mu$ L of 2  $\mu$ g/mL TMT0, TMT6, or TMT10 reagent in anhydrous acetonitrile. The reaction proceeded for 1 h then was quenched with hydroxylamine to a final concentration of 0.5%. For media amino acid analysis, 4  $\mu$ L of a stock of 20 amino acids (10 pmol/ $\mu$ L) labeled with TMT0 was mixed with media samples labeled with TMT6 (126 reagent). For 10-plex intracellular metabolite analysis, the 10 cell line samples were labeled and mixed equally and 4  $\mu$ L of the TMT0 stock was then mixed with the sample. For all experiments, mixed samples were diluted 1:100 in 0.1% formic acid for LC-MS. Glucose and lactate in the media were determined using the Yellow Springs Instrument (YSI) 7100 (Yellow Springs, OH).

**Protein Extraction, Digest, Labeling, and Fractionation.** Cell culture plates (15 cm) were rinsed with PBS, and cells were scraped in 2 mL of 2% SDS and 50 mM HEPES (pH 8.5), containing one tablet of complete mini protease inhibitor cocktail (Roche, Madison, WI) per 10 mL of lysis buffer. Lysates were homogenized with an Omni homogenizer (Kennesaw, GA) at the highest speed setting for 12 s per sample. Cysteine residues were reduced with 5 mM DTT and alkylated with 14 mM iodoacetamide followed by methanol-chloroform precipitation. Precipitated protein was resolubilized in 6 M guanidine-HCl and 50 mM HEPES (pH 8.5), and protein content was measured using a BCA assay (Thermo Scientific, Rockford, IL). An aliquot of 50  $\mu$ g of protein from each sample was diluted to 2 M guanidine-HCl with 50 mM HEPES (pH 8.5) and digested for 2 h with endoproteinase Lys-C (Wako, Japan) at a ratio of 1:200 Lys-C/protein. Samples were further digested overnight with trypsin (Promega, Madison, WI) at a ratio of 1:100 trypsin/protein. The digest was acidified with formic acid to a pH < 3, and peptides were desalted using 50 mg of solid-phase C18 extraction cartridges (Waters, Millford, MA), followed by lyophilization. Samples were resuspended in 100  $\mu$ L of 200 mM HEPES (pH 8.5) and 30% ACN. To each sample, 10  $\mu$ L of 20  $\mu$ g/mL 10-plex TMT reagents in anhydrous acetonitrile was added. The reaction proceeded for 1 h and then was quenched with hydroxylamine to a final concentration of 0.5%. Samples were then combined equally, desalted using 50 mg of solid-phase C18 extraction cartridge (Waters, Millford, MA), and then lyophilized. Basic-pH reversed-phase chromatography was used to fractionate the labeled peptide sample using an Agilent 300-Extend, 4.6 mm  $\times$  250 mm, 5  $\mu$ m C18 column (Agilent, Santa Clara, CA). A gradient of 5% to 40% acetonitrile (10 mM ammonium formate, pH 8) was applied at a flow rate of 800  $\mu$ L/min using an Agilent 1100 pump. Fractions were collected every 0.38 min, beginning at 10 min; then, every 12th fraction was combined to a single sample creating 12 fractions. Eight representative fractions were desalted using homemade stage-tips as previously described<sup>11</sup> and lyophilized.

**LC-MS and Data Analysis of Labeled Amino Acids.** For MS1-level analyses, all labeled amines were analyzed using an Orbitrap Exactive mass spectrometer (Thermo Fisher Scientific, San Jose, CA) coupled with a Thermo-Pal autosampler (Thermo Fisher Scientific, San Jose, CA) and an Accela 600 LC pump (Thermo Fisher Scientific, San Jose, CA). Chromatography was performed using a 100  $\mu$ m  $\times$  12 cm column, self-packed with 0.5 cm of Magic C4 resin (5  $\mu$ m particle size, Michrom Bioresources, Auburn, CA) and 12 cm of Maccel C18 AQ resin (3  $\mu$ m particle size, Nest Group, Southborough, MA). An injection volume of 4  $\mu$ L was used, and a gradient of 2% to 70% ACN (0.1% formic acid) over 15 min was used to separate compounds at a flow rate of 200 nL/min. The mass spectrometer scan range was 295–450  $m/z$  for amino acids, but for determining broader classes of labeled amines, the scan range was set to 295–1200  $m/z$ . All MS-1 analyses were conducted in positive ion mode using an AGC setting of  $3 \times 10^6$ , a resolution setting of  $5 \times 10^5$ , and a maximum injection time of 50 ms. Internal calibration was achieved using lock mass values of 371.10124 and 445.12003 as previously described.<sup>12</sup> LC-MS data were converted to mzXML format using a modified version of ReadW.exe and analyzed using the metabolomics software, Maven.<sup>13</sup> Peaks for TMT-labeled amines were identified using extracted ion chromato-

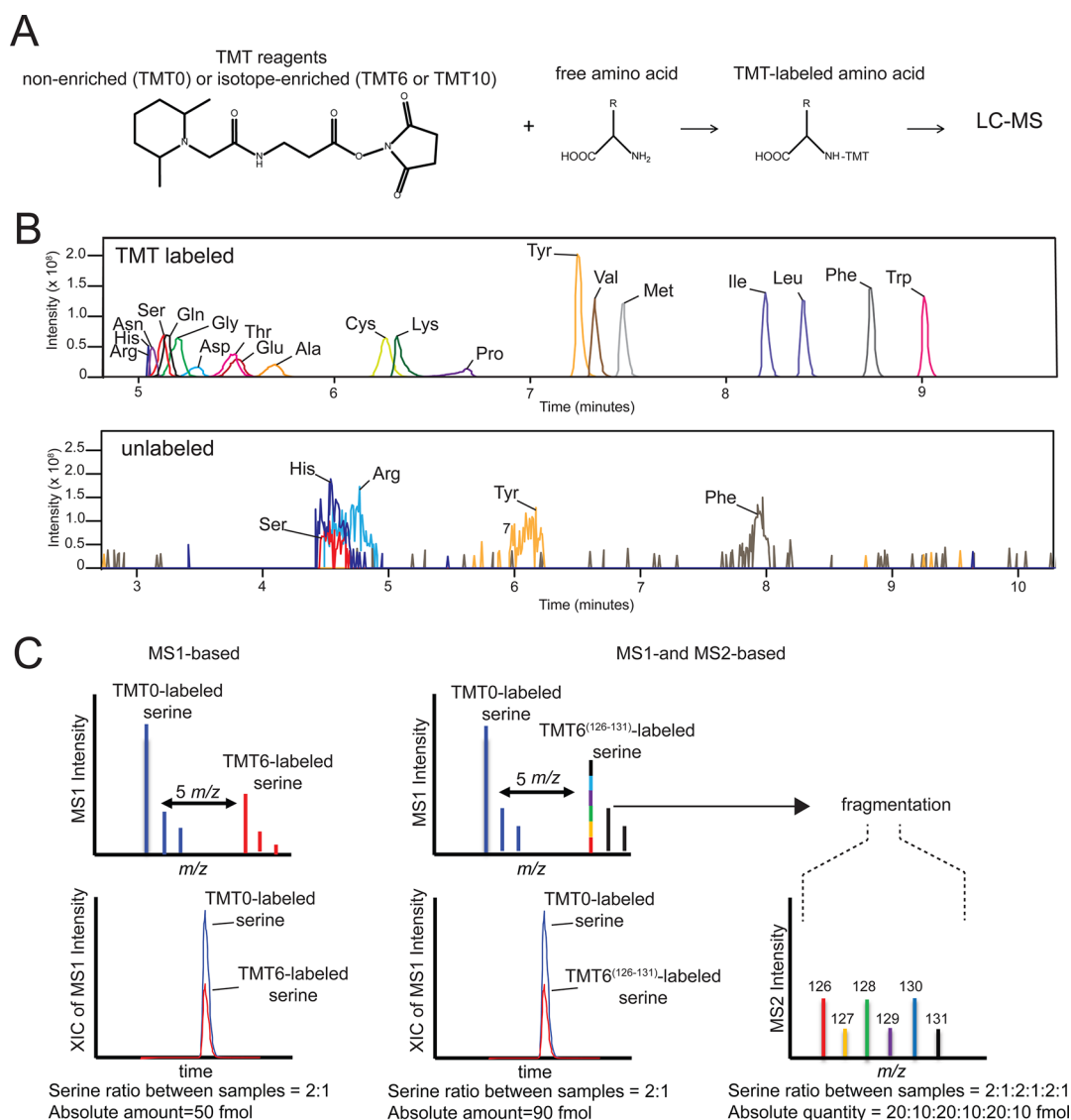


**Figure 1.** TMT labeling facilitates sensitive and versatile amino acid measurements by reversed-phase LC-MS. (A) Labeling scheme. TMT reagents, available as nonenriched (TMT0) or isotope-enriched (TMT6 or TMT10), react with free amines in amino acid standard preparations or methanol extracts of media or tissues. (B) Enhanced sensitivity of TMT-labeled amino acids for reversed-phase LC-MS. Standards of the 20 proteinogenic amino acids (10 pmol/ $\mu$ L) were either labeled with TMT0 or left unlabeled. Samples were diluted in 0.1% formic acid, and 100 fmol was analyzed by reversed-phase LC-MS. Shown are the extracted ion chromatograms of the TMT0-labeled and unlabeled amino acid forms. (C) Potential MS approaches to measure TMT-labeled amino acids and other amines. Two samples can be compared using MS1-based comparison of TMT0 and TMT6. Six to ten samples can be compared by using isobaric tags (TMT6<sup>126-131</sup> or TMT10<sup>126-131</sup>) with MS2-based reporter ions. For both of these approaches, TMT0-labeled internal standards can be used for absolute quantitation. Serine is used here to exemplify the approaches.

grams based on predicted masses for TMT-labeled amines from a published list<sup>14</sup> with a tolerance of 5 ppm.

#### LC-MS2 and Data Analysis of Labeled Amino Acids.

For MS2-level multiplexed analyses of amino acids, we used a Q-Exactive mass spectrometer (Thermo Fisher Scientific, San Jose, CA) coupled to a Famos autosampler and an Accella 600 LC pump (Thermo Fisher Scientific, San Jose, CA). Chromatography was performed using a 100  $\mu$ m  $\times$  12 cm column self-packed with 0.5 cm of Magic C4 resin (5  $\mu$ m particle size, Michrom Bioresources, Auburn, CA) and 12 cm of Maccel C18 AQ resin (3  $\mu$ m particle size, Nest Group, Southborough, MA). An injection volume of 4  $\mu$ L was used, and a gradient of 2% to 70% ACN (0.1% formic acid) over 30 min was used to separate compounds at a flow rate of 200 nL/min. MS1 was performed using a scan range of 295–450  $m/z$ , collision energy of 35, maximum injection time of 10 ms, and

resolution of  $6 \times 10^4$ . Amino acids were selected for fragmentation to detect their reporter ions using an inclusion list of expected TMT-labeled  $m/z$  for the 20 proteinogenic amino acids. MS2 were collected using HCD with a minimum threshold of 500 counts and a resolution setting of  $3 \times 10^4$ . Raw files were converted to mzXML format using a modified version of ReadW.exe. Peak areas of the MS1 for TMT0 and TMT10 were analyzed using Maven<sup>13</sup> and used to calculate the total amount of each amino acid from all 10 cell line samples (based on the TMT0 20 amino acid stock). MS2 scans for each amino acid were extracted with an in-house tool and using the TMT0-labeled version to determine proper retention time for TMT10 MS2 scans. For each amino acid, the sum of the reporter ion S/N values was converted to a percentage of the total for all 10 samples. These percentages were then used to

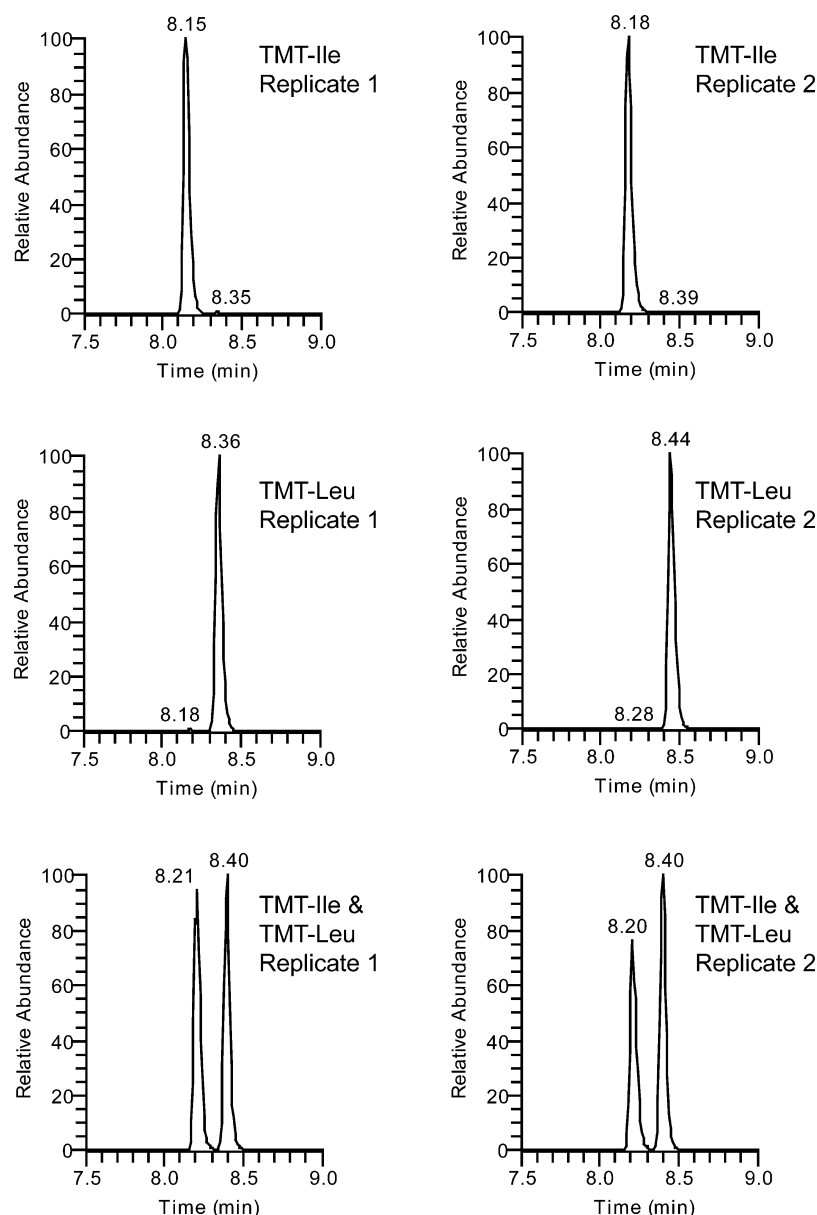


**Figure 2.** Separation of leucine and isoleucine by reversed-phase chromatography after TMT-labeling. Standards of leucine and isoleucine (1 pmol) were labeled individually with TMT0 and (in duplicate) 10 fmol of each was analyzed by LC-MS either individually or together.

calculate amino acid amounts based on the total (TMT0-calibrated) amount.

**LC-MS3 and Data Analysis of 10-Plex Quantitative Proteomics.** Each basic-pH reversed-phase fraction was resuspended in 0.1% formic acid and analyzed on an Orbitrap Elite (Thermo Fisher Scientific, San Jose, CA) using an Orbitrap LC-MS3 method as described previously.<sup>15</sup> Briefly, the top 10 precursor ions in each MS1 scan were selected for fragmentation and generation of an MS2 scan (used for peptide identification), from which multiple MS2 precursors were selected for an MS3 scan (used for reporter ion quantification). Spectra were matched against a Uniprot database (downloaded August, 2011) of human proteins, and protein false discovery rate was controlled to less than 1% using the reverse-database strategy.<sup>16</sup> Reporter ion S/N for all peptides matching each protein were summed, and protein relative expression values were represented as a fraction of the total intensity for all TMT reporter ions for the protein. Proteins that were uniquely

expressed at either high or low levels for each cell line were determined using a Euclidian distance metric to rank protein similarity to a given expression pattern (e.g., highly expressed only in both replicates of MCF10A cells). The top 50-ranked proteins for each pattern (high or low) were submitted to DAVID bioinformatics tool (<http://david.abcc.ncifcrf.gov>) to perform functional clustering and assign over-represented GO terms to each group of proteins. GO terms meeting Bonferroni-corrected  $p$ -values <0.05 were considered as over-represented.

## RESULTS AND DISCUSSION

Here, we have employed amine-reactive TMT reagents to derivatize amino acids and enhance their analysis by LC-MS. The TMT0 reagent is not enriched in stable isotopes and thus differs in mass from the traditional TMT reagents by 5 Da facilitating MS1-based quantitation when compared to TMT6 or TMT10 reagents (Figure 1A). To determine whether TMT-labeling of amino acids could facilitate their analysis by



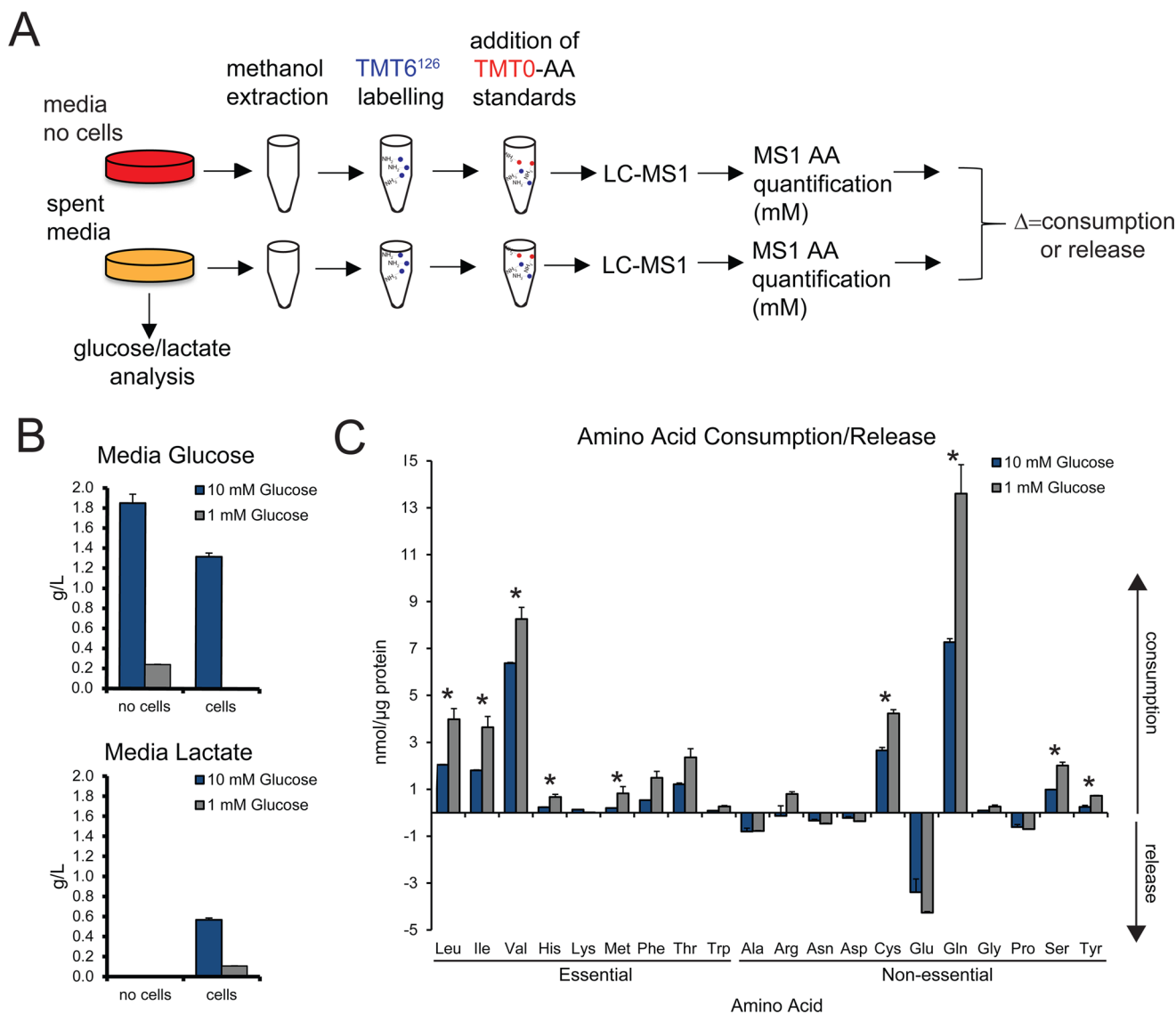


**Figure 3.** Amino acid consumption or release in a breast cancer cell line using MS1-based measurements of TMT-labeled amino acids. (A) Procedure for measuring amino acid uptake. Media samples were extracted by diluting 4-fold in 80% methanol followed by centrifugation. Supernatant was diluted 3-fold in 50 mM TEAB buffer (pH 8.5) and labeled with a single TMT6 reagent (126 reporter ion version). Amino acid amounts were determined by mixing with known quantities of TMT0-labeled amino acids followed by LC-MS analysis. Amino acid amounts in spent media were subtracted from control media (no cells) to determine consumption or release. (B) MDA-MB-231 cells were seeded overnight in high glucose DMEM and then switched to 10 or 1 mM glucose media. After 24 h, glucose and lactate analysis of the media by YSI showed complete glucose depletion and conversion to lactate in the 1 mM glucose-grown cells. (C) Media was measured using TMT labeling and LC-MS as outlined in panel (A). Amino acid consumption (+ values) or release (– values) from MDA-MB-231 cells in normal (10 mM glucose) versus glucose-limited (1 mM glucose) media is shown. \**t* test  $p < 0.05$ .

reversed-phase LC-MS analysis, we labeled 20 amino acid standards with TMT0 and analyzed the mixture (100 fmol of each amino acid) by LC-MS. As a comparison, an equivalent amount of 20 unlabeled amino acid standards was also analyzed. While the unlabeled forms of amino acids gave poor signal and peak shape, all 20 TMT-labeled forms of amino acids were detected, most with drastically improved peak shape and decreased peak width (Figure 1B). Although difficult to assess improvements in sensitivity imparted by TMT labeling since many unlabeled amino acids are not detected, increases in sensitivities observed here are similar to those reported using DiART tags (>20-fold on average).<sup>8</sup> These improvements are likely a result of improved ionization efficiency and hydrophobicity imparted by the TMT reagent and an  $m/z$  shift to a

cleaner mass range than is typical of the unlabeled amino acids. There are multiple quantitative amino acid analysis strategies whereby TMT-labeling could be employed using MS1- or MS2-based LC-MS (Figure 1C). In these strategies, TMT0 can be combined with TMT6 or TMT10, significantly extending the capabilities provided by other amine labeling approaches, allowing absolute quantitation and multiplexing with 10 samples. We also noticed that TMT-labeling of amino acids provided baseline chromatographic separation of peaks for the isobaric amino acids leucine and isoleucine. To distinguish leucine peaks from isoleucine, we analyzed standards of each amino acid alone, or as a mixture, and observed consistent elution of isoleucine (retention time = 8.15 to 8.21 min) prior to leucine (retention time = 8.36 to 8.44 min) (Figure 2). As

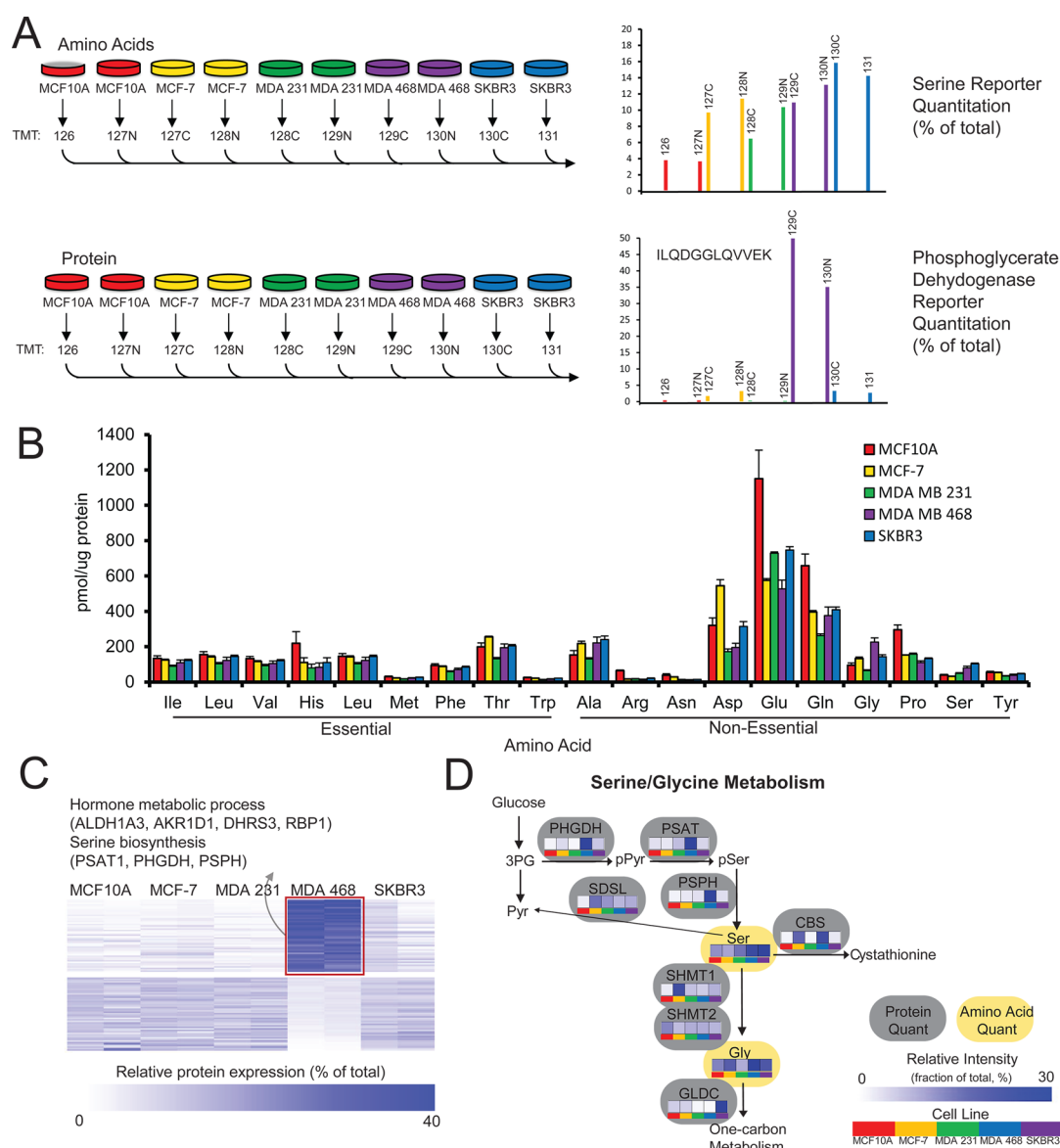


**Figure 4.** Isobaric TMT labeling allows multiplexed quantitation of proteins and amino acids in parallel. (A) Setup of amino acid and proteomics experiments. For amino acid analysis, 5 breast epithelial cell lines were extracted in 80% methanol (in duplicate) and labeled using isobaric 10-plex TMT reagents (TMT10<sup>126–131</sup>) and then analyzed by a targeted LC-MS2 method in triplicate. Absolute levels were determined using TMT0-labeled amino acids as internal standards. For proteomics, a data set was collected from the same 5 cell lines in duplicate, using isobaric 10-plex TMT reagents (TMT10<sup>126–131</sup>) and analyzed by a 2D-LC-MS3 method. Reporter ion quantitation of amino acids and protein expression is exemplified here by serine and phosphoglycerate dehydrogenase (a serine biosynthetic enzyme). (B) Comparison of intracellular amino acid levels between the 5 breast cancer cell lines achieved using 10-plex isobaric labeling. Error bars are the standard error of the mean ( $n = 2$  biological duplicates  $\times$  3 technical triplicates) for each cell line. (C) Functional analysis of proteins elevated in specific cell lines from the 10-plex proteomics data set reveals significant over-representation of serine biosynthesis in MDA-MB-468 cells. (D) Comparative proteomic and amino acid data across cell lines overlaid in the pathway format for the glycine/serine biosynthetic pathway.

such, TMT-labeling and reversed-phase LC-MS can be used to detect all 20 proteinogenic amino acids.

Large-scale consumption and release measurements have recently been employed to show that glycine utilization correlates with cell proliferation.<sup>17</sup> On the basis of these findings, we propose that our method using TMT could be valuable in determining amino acid consumption from cell culture media. We thus employed an MS1-based duplex labeling strategy whereby a set of 20 amino acid standards was labeled with TMT0 to generate a 10 pmol/ $\mu$ L stock which could be used to internally calibrate and calculate TMT6-labeled media amino acid amounts. Samples were analyzed by

nanoflow reversed-phase LC-MS using a standalone Orbitrap, and amino acid amounts based on LC-MS peak areas were then determined. Spent media amounts were subtracted from control media amounts (with no cells) to determine consumption or release (Figure 3A). We demonstrated this approach by determining amino acid consumption or release in highly glycolytic MDA-MB-231 breast cancer cells during glucose-starvation (Figure 3B,C). We observed significantly greater consumption of most amino acids in glucose-starved versus unstarved cells (Figure 3C). The most pronounced increase in consumption (1.9-fold) was for glutamine, which was accompanied by increased glutamate release (Figure 3C).

Glutamine is an important fuel source for anabolic pathways in cancer cells,<sup>18</sup> so it is not surprising that these glucose-deprived cells increased glutamine consumption. Amino acid consumption and release observed in this experiment are similar to those in the recent large-scale consumption and release data set for MDA-MB-231 cells, whereby the majorly consumed amino acid was glutamine, with concomitant glutamate release.<sup>17</sup>

Toward determining intracellular amino acid measurements, we first explored the detection of intracellular amines by LC-MS after TMT labeling. We labeled an 80% methanol extract of MCF-7 breast cancer cells with TMT0 and matched LC-MS peaks against amine-containing metabolites from a published list of 137 human central carbon metabolites<sup>14</sup> (ppm tolerance = 5 ppm). The most abundantly detected peaks were observed for amino acids, although several other amine-containing species were matched to the list, including relatively unstudied metabolites such as taurine and *N*-acetylputrescine (Table S-1, Supporting Information). Although other primary amine-containing metabolites exist in cells, their detection was not the focus of these analyses. The metabolites we detected here are similar, however, to studies whereby amines in cell lines were tagged using either iTRAQ,<sup>6</sup> Acq,<sup>7</sup> or DiART.<sup>8</sup> Taken together, these results indicate that, although many putative amine metabolites are present, amino acids and several other related amines dominate the amine metabolite profile of cultured cells. Analysis of other sample types such as plasma and other bodily fluids may reveal a greater number of amine metabolites. Indeed, analysis of amines in saliva by others using dansylation derivatization of amines revealed a large number of putative amine features but were mostly unidentified.<sup>19</sup>

We next utilized 10-plex isobaric labeling reagents (Figure S-1, Supporting Information) to perform multiplexed analysis of amino acids, comparing 5 different breast cancer cell lines: MCF10A (basal-like, nontumorigenic), MCF-7 (luminal A, estrogen receptor positive, progesterone receptor positive), MDA-MB-231 (basal, triple negative), MDA-MB-468 (basal, triple negative, overexpressing EGFR), and SKBR3 (overexpressing ERBB2). Cell line samples were prepared in biological duplicates among the 10 TMT labels, injecting each sample in triplicate (Figure 4A). For amino acid quantitation, the total amount of each amino acid in all samples was estimated on the basis of the internal-calibrant stock solution of TMT0-labeled amino acid standards mixed with the samples (as shown in Figure 1C). During LC-MS2 data collection, amino acid *m/z* values were targeted using an inclusion list to generate reporter ions. Reporter ion S/N values were summed within each TMT10 channel (126–131, illustrated in Figure S-1, Supporting Information) and used to estimate the fraction of the total amount of each amino acid in each cell line sample. We observed glutamine and glutamate to be the most abundant amino acids in most of the cell lines (Figure 4B), whereas aspartate was the most abundant in MCF-7 cells. Comparing between cell lines, we observed the nontumorigenic cell line (MCF10A) to have comparatively higher levels of glutamine and glutamate than others and MDA-MB-468 and SKBR3 had comparatively higher levels of serine (Figure 4B). We observed the amino acids methionine, tryptophan, arginine, and asparagine to be among the least abundant amino acids in the breast cancer cell lines used here. Unfortunately, cysteine did not give sufficient MS1 signal to trigger MS2 acquisition.

In parallel to the amino acid data, we also generated a 10-plex quantitative proteomics data set for the same 5 breast cancer

cell lines in duplicate (Figure 4A). Here, we were mainly interested in generating a data set with good coverage of the major amino acid metabolism pathways, but many other proteins were measured (Table S-2, Supporting Information). To interpret cell line differences, we extracted proteins that were expressed at specifically high or low levels in a single cell line (Table S-2, Supporting Information) and submitted them to DAVID bioinformatics resource<sup>19</sup> for GO term enrichment analysis (Figure S-2B, Supporting Information). In terms of amino acid metabolism, we observed significant amino acid GO term differences in MDA-MB-468 cells, which were particularly unique in their elevated expression of GO terms representing the serine and glycine biosynthesis pathway: 3-phosphoglycerate dehydrogenase (PHGDH), phosphoserine aminotransferase (PSAT), phosphoserine phosphatase (PSPH), and cystathionine beta-synthase (CBS) (Figure 4C and Figure S-2B, Supporting Information). Aligning quantitative proteomic data for the serine/glycine biosynthetic pathway, we observe slightly more serine and glycine in correlation with PHGDH, PSAT, PSPH, and CBS (Figure 4D). It has recently been shown that some breast and skin cancer cell lines, including MDA-MB-468 cells, are dependent on amplification of the glycine/serine biosynthetic pathway whereby glucose carbons are directed toward amino acid synthesis.<sup>20,21</sup> Although serine biosynthesis was the most profound change in these cells, other amino acid pathways are shown with replicate analyses in Figure S-3, Supporting Information. We also find that MCF10A cells had higher expression of GLUD1 (Table S-2, Supporting Information) which is a key protein involved in glutamine utilization and correlates with the higher levels of glutamine and glutamate observed in these cells (Figure 4B) suggesting a reliance on this pathway. We propose that, although collected with minimal fractionation such that it is not completely comprehensive, the proteomic data set (Table S-2, Supporting Information) could be used to inform upon proteins in breast cancer.

We further incorporated amino acid and proteomic data to correlate amino acid metabolism with molecular features important in oncogenesis. Although we collected the proteomics data set to profile differences in amino acid metabolism proteins, we were able to compare several important cancer-related proteins from the data set (Table S-2, Supporting Information) and correlate them with amino acid metabolism. We observed elevated glycine in MDA-MB-468 cells, which correlated with epithelial growth factor receptor (EGFR) (Figure 4B and Figure S-2A, Supporting Information). These results are interesting in light of recent findings that glycine consumption is correlated with cell proliferation in multiple cell lines and suggests that EGFR may play a role in elevated serine/glycine biosynthesis.<sup>22</sup> It is currently unclear how the serine biosynthesis pathway is elevated in these cells but, it may be controlled by EGFR based on our observations. We also observed a correlation between ERBB2, in SKBR3 cells, with elevated GLDC (Figure 4B and Figure S-2A, Supporting Information), which is an important protein regulating glycine cleavage toward one-carbon and folate metabolism in proliferating cells.<sup>4</sup> The signaling kinase, AKT1, correlated with aspartate levels in MCF-7 cells (Figure 4B and Figure S-2A, Supporting Information) and may play a role in regulation of aspartate levels. Although these correlates remain to be validated, they provide directions for new hypotheses in metabolic regulation.

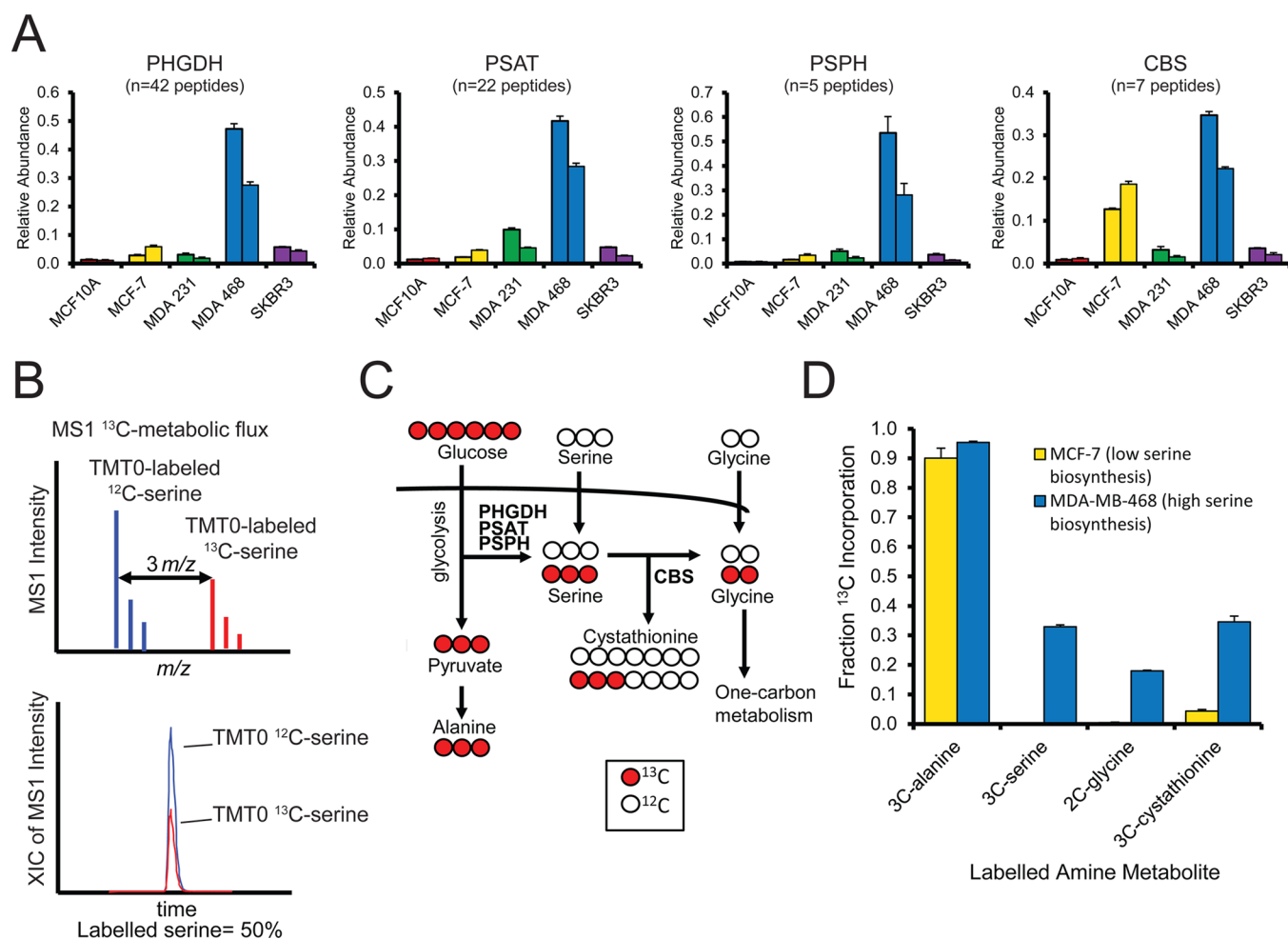


**Figure 5.** Analysis of glycine/serine metabolism by TMT-labeling reveals glucose incorporation to cystathionine and elevated glycine/serine metabolism proteins. (A) Relative abundance, based on the 10-plex TMT quantitative proteomics data set, for serine, glycine, and cystathionine metabolism pathway proteins. Error bars are the standard error of the mean peptide relative abundances for each protein (number of peptides is shown in the inset). (B) Example MS1 spectra and corresponding XICs for TMT0-labeled, natural, and  $^{13}\text{C}$ -glucose-derived versions of serine. (C) Major routes of labeled glucose carbon incorporation into alanine, glycine, serine, and cystathionine. (D)  $^{13}\text{C}$ -glucose-carbon incorporation measured by TMT labeling of amines. MCF-7 and MDA-MB-468 cells (with differing levels of glycine/serine metabolism proteins) were grown for 48 h in fully  $^{13}\text{C}$ -labeled glucose. Methanol extracts were labeled with TMT0 and analyzed by LC-MS. Peaks were detected and measured for  $^{13}\text{C}$ -labeled alanine, serine, glycine, and cystathionine revealing, for each of these pools, the fraction originating from glucose.

We next determined whether TMT labeling could be employed to detect glucose flux to amine metabolites in cultured cells (as outlined in Figure 5B,C). We chose to compare MCF-7 and MDA-MB-468 cells since the quantitative proteomics data set revealed that MDA-MB-468 cells have amplified levels of serine biosynthesis proteins PHGDH, PSAT, and PSPH, whereas MCF-7 cells have very low levels of these proteins but elevated levels of CBS (Figure 5A). These proteins are important in redirecting glucose carbons from glycolysis into serine and glycine synthesis<sup>20</sup> and possibly into cystathionine, a precursor to cysteine-related redox metabolism (Figure 5C). MCF-7 and MDA-MB-468 cells were grown in 10 mM fully  $^{13}\text{C}$ -labeled glucose for 48 h, and methanol extracts were labeled with TMT0. Glucose uptake and lactate release for these 2 cell lines are similar (Figure S-4, Supporting Information). For amino acids gaining 2 carbons from glucose (e.g. glycine), quantification of the metabolically labeled  $^{213}\text{C}$  peaks may be interfered with from the naturally abundant  $^{13}\text{C}$  peaks. We show, however, that this effect is minimal for TMT0-labeled glycine (Figure S-5, Supporting Information). We observed significant levels of  $^{313}\text{C}$ -alanine in both cell lines in

which more than 90% of the alanine pool was  $^{313}\text{C}$ -labeled (Figure 5D). The presence of  $^{313}\text{C}$ -serine and  $^{213}\text{C}$ -glycine was correlated with the expression of PHGDH, PSAT, and PSPH, where in MDA-MB-468 cells, the  $^{313}\text{C}$ -serine and  $^{213}\text{C}$ -glycine pools were, on average, 32% and 18%, respectively, but undetectable in MCF-7 cells (Figure 5D). We also detect  $^{313}\text{C}$ -cystathionine in both cell lines, where in MDA-MB-468 and MCF-7 cells, it made up 35% and 4% of the total cystathionine pools, respectively (Figure 5D). It is unclear if carbon follows the same route from glucose to cystathionine in both cell lines since we do not observe glucose-labeled serine and glycine in MCF-7 cells. Although cystathionine is a precursor to cysteine, we do not detect labeled cysteine in either cell line. These data suggest glucose carbon might be directed toward cystathionine biosynthesis to maintain redox metabolism. We did not detect  $^{13}\text{C}$  incorporation to any other amino acids.

## CONCLUSION

Derivatization with TMT reagents allows for enhanced amino acid analyses using reversed-phase LC-MS. This approach



facilitates parallel quantitative analysis of both proteins and amino acids with similar LC-MS setups. This approach is applicable to measuring flux of glucose to amino acids, which is a very important phenomenon in many cancers. By providing a highly multiplexed assay, TMT labeling of amino acids could be easily incorporated into screening strategies to find therapeutic targets for dysregulated amino acid metabolism in cancer. We also propose that TMT labeling could be used for sensitive quantitation of circulating amino acids as markers of genetic diseases like phenylketonuria as well as detection of biogenic amines such as dopamine and serotonin. The method can be scaled to use minimal sample amounts and reagent quantities making the approach economical for most laboratories, providing a new tool for exploring cellular metabolic regulation.

## ■ ASSOCIATED CONTENT

### Supporting Information

Additional information as noted in text. This material is available free of charge via the Internet at <http://pubs.acs.org>.

## ■ AUTHOR INFORMATION

### Corresponding Authors

\*E-mail: [pat\\_murphy@hms.harvard.edu](mailto:pat_murphy@hms.harvard.edu).

\*E-mail: [sgygi@hms.harvard.edu](mailto:sgygi@hms.harvard.edu).

### Notes

The authors declare no competing financial interest.

## ■ ACKNOWLEDGMENTS

The authors wish to acknowledge Joao Paulo for help with instrumentation for MS2 analysis of tagged amino acids. We also acknowledge Brian Erickson, Deepak Kolippakkam, and Ed Huttlin for the in-house protein profile matching tool and bioinformatics analysis. This work was funded in part by a grant from the NIH (GM67945).

## ■ REFERENCES

- (1) Patti, G. J.; Yanes, O.; Siuzdak, G. *Nat. Rev. Mol. Cell Biol.* **2012**, *13*, 263–269.
- (2) Blau, N.; van Spronsen, F. J.; Levy, H. L. *Lancet* **2010**, *376*, 1417–1427.
- (3) Simon, E.; Flaschker, N.; Schadowaldt, P.; Langenbeck, U.; Wendel, U. *J. Inherited Metab. Dis.* **2006**, *29*, 716–724.
- (4) Locasale, J. W. *Nat. Rev. Cancer* **2013**, *13*, 572–583.
- (5) Kaspar, H.; Dettmer, K.; Gronwald, W.; Oefner, P. J. *Anal. Bioanal. Chem.* **2009**, *393*, 445–452.
- (6) Kaspar, H.; Dettmer, K.; Chan, Q.; Daniels, S.; Nimkar, S.; Daviglus, M. L.; Stamler, J.; Elliott, P.; Oefner, P. J. *J. Chromatogr., B* **2009**, *877*, 1838–1846.
- (7) Boughton, B. A.; Callahan, D. L.; Silva, C.; Bowne, J.; Nahid, A.; Rupasinghe, T.; Tull, D. L.; McConville, M. J.; Bacic, A.; Roessner, U. *Anal. Chem.* **2011**, *83*, 7523–7530.
- (8) Yuan, W.; Zhang, J.; Li, S.; Edwards, J. L. *J. Proteome Res.* **2011**, *10*, 5242–5250.
- (9) Yuan, W.; Anderson, K. W.; Li, S.; Edwards, J. L. *Anal. Chem.* **2012**, *84*, 2892–2899.
- (10) Thompson, A.; Schafer, J.; Kuhn, K.; Kienle, S.; Schwarz, J.; Schmidt, G.; Neumann, T.; Hamon, C. *Anal. Chem.* **2003**, *75*, 1895–1904. Ross, P. L.; Huang, Y. N.; Marchese, J. N.; Williamson, B.; Parker, K.; Hattan, S.; Khainovski, N.; Pillai, S.; Dey, S.; Daniels, S. *Mol. Cell. Proteomics* **2004**, *3*, 1154–1169.
- (11) Rappsilber, J.; Ishihama, Y.; Mann, M. *Anal. Chem.* **2003**, *75*, 663–670.
- (12) Haas, W.; Faherty, B. K.; Gerber, S. A.; Elias, J. E.; Beausoleil, S. A.; Bakalarski, C. E.; Li, X.; Villen, J.; Gygi, S. P. *Mol. Cell. Proteomics* **2006**, *5*, 1326–1337.
- (13) Melamud, E.; Vastag, L.; Rabinowitz, J. D. *Anal. Chem.* **2010**, *82*, 9818–9826.
- (14) Lu, W.; Clasquin, M. F.; Melamud, E.; Amador-Noguez, D.; Caudy, A. A.; Rabinowitz, J. D. *Anal. Chem.* **2010**, *82*, 3212–3221.
- (15) McAlister, G. C.; Huttlin, E. L.; Haas, W.; Ting, L.; Jedrychowski, M. P.; Rogers, J. C.; Kuhn, K.; Pike, I.; Grothe, R. A.; Blethrow, J. D. *Anal. Chem.* **2012**, *84*, 7469–7478.
- (16) Elias, J. E.; Gygi, S. P. *Nat. Methods* **2007**, *4*, 207–214.
- (17) Jain, M.; Nilsson, R.; Sharma, S.; Madhusudhan, N.; Kitami, T.; Souza, A. L.; Kafri, R.; Kirschner, M. W.; Clish, C. B.; Mootha, V. K. *Science* **2012**, *336*, 1040–1044.
- (18) DeBerardinis, R. J.; Mancuso, A.; Daikhin, E.; Nissim, I.; Yudkoff, M.; Wehrli, S.; Thompson, C. B. *Proc. Natl. Acad. Sci.* **2007**, *104*, 19345–19350.
- (19) Zheng, J.; Dixon, R. A.; Li, L. *Anal. Chem.* **2012**, *84*, 10802–10811.
- (20) Huang, D. W.; Sherman, B. T.; Lempicki, R. A. *Nat. Protoc.* **2008**, *4*, 44–57.
- (21) Possemato, R.; Marks, K. M.; Shaul, Y. D.; Pacold, M. E.; Kim, D.; Birsoy, K.; Sethumadhavan, S.; Woo, H. K.; Jang, H. G.; Jha, A. K. *Nature* **2011**, *476*, 346–350.
- (22) Locasale, J. W.; Grassian, A. R.; Melman, T.; Lyssiotis, C. A.; Mattaini, K. R.; Bass, A. J.; Heffron, G.; Metallo, C. M.; Muranen, T.; Sharfi, H. *Nat. Genet.* **2011**, *43*, 869–874.